
Article:
Himmelberg, Marc Mason orcid.org/0000-0001-9133-7984, West, Ryan John Hatcher, Elliott, Christopher John Hazell orcid.org/0000-0002-5805-3645 et al. (1 more author) (2018) Abnormal visual gain control and excitotoxicity in early-onset Parkinson's disease Drosophila models. Journal of Neurophysiology. jn.00681.2017. pp. 957-970. ISSN 0022-3077

https://doi.org/10.1152/jn.00681.2017

Articles in PresS. J Neurophysiol (November 15, 2017). doi:10.1152/jn.00681.2017

Abnormal visual gain control and excitotoxicity in early-onset Parkinson's disease Drosophila models

Marc M. Himmelberg[1*], Ryan J.H. West[2], Christopher J.H. Elliott[2], and Alex R. Wade[1]

[1] Department of Psychology, The University of York, York

[2] Department of Biology, The University of York, York

*Corresponding author

Abbreviated title/running head: GAIN CONTROL AND EXCITOTOXICITY IN PD MODELS

Address for correspondence: M.M. Himmelberg, Department of Psychology, University of York, York, United Kingdom, YO10 4DD (email: marchimmelberg@gmail.com)

Abstract

The excitotoxic theory of Parkinson's disease (PD) hypothesises that a pathophysiological degeneration of dopaminergic neurons stems from neural hyperactivity at early stages of disease, leading to mitochondrial stress and cell death. Recent research has harnessed the visual system of Drosophila PD models to probe this hypothesis. Here, we investigate whether abnormal visual sensitivity and excitotoxicity occur in early-onset PD (EOPD) Drosophila models DJ-1$\alpha^{\Delta 72}$, DJ1-$\beta^{\Delta 93}$, and PINK1^{5}. We used an electroretinogram to record steady state visually evoked potentials driven by temporal contrast stimuli. At 1 day of age, all EOPD mutants had a twofold increase in response amplitudes when compared to w^{-} controls. Further, we found that excitotoxicity occurs in older EOPD models after increased neural activity is triggered by visual stimulation. In an additional analysis, we used a linear discriminant analysis to test whether there were subtle variations in neural gain control that could be used to classify Drosophila into their correct age and genotype. The discriminant analysis was highly accurate, classifying Drosophila into their correct genotypic class at all age groups at 50-70% accuracy (20% chance baseline). Differences in cellular processes link to subtle alterations in neural network operation in young flies – all of which lead to the same pathogenic outcome. Our data are the first to quantify abnormal gain control and excitotoxicity in EOPD Drosophila mutants. We conclude that EOPD mutations may be linked to more sensitive neuronal signalling in prodromal animals that may cause the expression of PD symptomologies later in life.

New and Noteworthy: SSVEP response amplitudes to multivariate temporal contrast stimuli were recorded in early-onset PD Drosophila models. Our data

indicate that abnormal gain control and a subsequent visual loss occur in these PD mutants, supporting a broader excitotoxicity hypothesis in genetic PD. Further, linear discriminant analysis could accurately classify Drosophila into their correct genotype at different ages throughout their lifespan. Our results suggest increased neural signalling in prodromal PD patients.

Keywords: Parkinson's disease, Gain Control, Excitotoxicity, SSVEPs, Drosophila, Linear Discriminant Analysis

Introduction

Parkinson's Disease (PD) is the second most common progressive neurodegenerative disorder, affecting ~0.2-3% of the population, with an increased prevalence in those aged over 50 (Clarke, 2007; de Rijk et al., 1997). PD is thought to stem from the pathophysiologic degeneration and subsequent loss of dopaminergic neurons within the pars compacta of the substantia nigra, a basal ganglia structure that plays a key role in movement (Clarke, 2007)**.** It is hypothesised that neuronal death in PD is caused by an excitotoxic mechanism, in which neuronal hyperactivity leads to neurodegeneration. Neuronal hyperactivity causes an increase in demand for ATP from mitochondria, leading to oxidative stress and eventual neuronal death (Beal et al., 1993; Surmeier, Obeso, & Halliday, 2017). In both mammals and invertebrates, neuronal responses are regulated by a tightly-linked network of excitatory and inhibitory gain control mechanisms that, collectively, we refer to as 'normalization' (Carandini & Heeger, 1994; Carandini, Heeger, & Movshon, 1997; Carandini & Heeger, 2011; Single, Haag, & Borst, 1997). Normalization mechanisms can be measured across the animal kingdom using a range of methods, including steady state visually evoked potential (SSVEP) recordings, a sensitive technique commonly used to measure the amplitude of neural population responses to periodic flickering stimuli (Busse, Wade, & Carandini, 2009; Norcia, Appelbaum, Ales, Cottereau, & Rossion, 2015; Regan, 1966; Tyler, Apkarian, & Nakayama, 1978).

In Drosophila, SSVEP recordings are collected from the surface of the eye and can be made in both healthy and PD mutant Drosophila (Afsari et al., 2014; West, Elliott, & Wade, 2015a). Previously we have shown that young flies carrying

the late-onset gain-of-function PD mutation LRRK2-G2019S showed increased visual contrast sensitivity to full field flicker stimuli, reflecting a failure in regulation of neural activity (i.e. abnormal gain control or normalization) at one day of age (Afsari et al., 2014). This regulatory failure is followed by a decline in visual function over time, with physiological and anatomical degeneration in older LRRK2-G2019S Drosophila (Hindle et al., 2013; Mortiboys et al., 2015).

Feeding LRRK2-G2019S Drosophila with BMPPB-32, a kinase inhibitor specifically targeted at LRRK2, restored normal contrast sensitivity at both 1 and 14 days of age, indicating that both the early neuronal hypersensitivity and the subsequent neurodegeneration are due to abnormal kinase domain activity (Afsari et al., 2014). Vision loss was accelerated by increasing neural activity via photic stimulation of the Drosophila visual system using flashing LED lights. Together, these findings support an excitotoxicity theory of the LRRK2-G2019S form of PD. This excitotoxicity theory of PD has also found support in rodent models of the G2019S mutation (Longo, Russo, Shimshek, Greggio, & Morari, 2014; Matikainen-Ankney et al., 2016; Ponzo et al., 2017; Sloan et al., 2016; Volta et al., 2017).

We have previously demonstrated that linear discriminant analysis (LDA) is a useful tool in the analysis of SSVEP data obtained from Drosophila (West, Elliott, & Wade, 2015b). Here, our findings indicated differences in SSVEP amplitude both between and within wild type flies and EOPD mutants, in response to spatiotemporal patterns. These differences had enough statistical regularity for LDA to accurately discriminate between genotypes. When compared to wild-type controls, qualitative observations indicated an elevation in SSVEP response in 1 day old EOPD flies.

Although LDA has diagnostic utility, it does not allow for the quantification of directional differences in such responses. Having established this method, we now seek to expand upon this and investigate abnormal gain control and excitotoxicity in EOPD models.

Is excitotoxicity a general feature of all Drosophila PD mutants? If so, it would suggest that rather than being an epiphenomenon of some metabolic dysfunction that causes PD, the excitotoxicity itself is central to the disease. In the current paper, we use SSVEP techniques combined with principal components analysis, general linear modelling, and multivariate classification analysis, to investigate abnormal gain control and excitotoxicity in EOPD Drosophila models. We hypothesised that abnormal gain control would occur in young Drosophila carrying EOPD mutations due to disease related changes in retinal dopaminergic neurons, reflected by increased SSVEP amplitudes in 1 day old EOPD Drosophila mutants. We also hypothesised that abnormal gain control would cause an excitotoxic cascade in older EOPD Drosophila. Consequently, we expected to observe a decrease in SSVEP amplitudes at later ages. Finally, we wondered if all mutations affected neuronal gain control in the same manner or if there were subtle mechanistic variations that could be used to differentiate the genotypes. To address this, we used linear discriminant analysis based on SSVEP responses to a range of temporal modulation rates and contrast levels to attempt to classify flies into their correct genotypic class at different points throughout their lifespan. The greater the differences in the gain control profiles across genotypes, the greater the accuracy we expected from this classification.

We found that SSVEP response amplitudes to spatial stimuli are significantly increased in EOPD mutants at 1 day of age – indicating that neuronal gain control is abnormal in these animals. Generating additional neuronal stress by exposing flies to randomly pulsating light for 7 days resulted in a profound loss of vision in all PD mutants, supporting the excitotoxicity model of PD. Finally, there are robust differences between the temporal contrast response profiles of the different PD mutants which allow our multivariate classification algorithms to classify flies into their respective genotypes at well above chance levels throughout their lifespan.

Materials and Methods

Drosophila stocks and maintenance

Drosophila were raised in a 12hr:12hr light:dark (LD) cycle at 25° on standard food consisting of agar (1% w/v), cornmeal (3.9%), yeast (3.7%), and sucrose (9.4%). All flies were outcrossed and stabilised where appropriate to remove any naturally occurring mutations. Three EOPD mutations (DJ-1$\alpha^{\Delta 72}$, DJ1-$\beta^{\Delta 93}$, and PINK1^{5}), one knockout of the fly LRRK2 homologue (dLRRK^{ex1}) and one wild-type control genotype (w^{1118}, herein w^{-}) were deployed. w^{-} strains were gifted by Sean Sweeney. PINK1^{5} and dLRRK^{ex1} strains were obtained from the Bloomington Drosophila Stock Centre (Indiana, USA), whilst DJ-1$\alpha^{\Delta 72}$ and DJ1-$\beta^{\Delta 93}$ strains were kind gifts from Alex Whitworth. Male flies all had white eyes, and were tested at 1, 7, 14, 21, and 28 days post eclosion.

Preparation of Drosophila for Testing

Male flies were collected within 8 hours of eclosion and transferred to a new vial of standard food that additionally contained nipagin (0.1% w/v). Flies were

maintained in these vials and transferred to fresh food weekly. Flies were kept in a 12hr:12hr LD cycle at 25℃ until they had reached appropriate age for testing.

Photic stress

To explore as to whether an increase in neural demand resulted in a decrease in SSVEP amplitudes, all Drosophila genotypes were exposed to a photic stressor condition (Afsari et al., 2014; Hindle et al., 2013). Male flies were collected within 8 hours of eclosion and transferred to a new vial of standard food containing nipagin. These flies were maintained within a 29℃ incubator with irregularly pulsating LED lights at ~1.5s intervals to force the Drosophila visual system to adapt to new light levels and increase photoreceptor response. Flies were maintained here for 7 days, as this was the age at which G2019S mutants had previously shown visual loss (Hindle et al., 2013). Ten flies of each genotype tested (except for DJ-1$\alpha^{\Delta 72}$ where eight were tested) (N=48).

Preparation for Electroretinogram

On the day of testing, flies were collected using a pooter and aspirated into a shortened pipette. Once the fly's head was protruding from the tip of the pipette, it was restrained by placing a small layer of nail varnish on the back of the fly's neck. Two pipettes at a time were mounted onto a customised Drosophila electroretinogram (ERG) recording system, with both flies placed 22cm away from the dual display monitors (West et al., 2015). ERG recordings were made through hollow drawn-glass electrodes containing simple saline (130mM, NcCl, 4.7 mM KCl, 1.9mM $CaCl_2$) connected to a high-impedance amplifier (LF356 op-amp in the circuit [Fig.7] of (Ogden, 1994)) via thin silver wires. The reference electrode was inserted

gently onto the Drosophila proboscis, and the recording electrode was placed on the surface of the right eye. Ten unique flies of each genotype at each age were tested (total N=250).

Stimuli

Stimuli were contrast-reversing achromatic sine wave gratings with a range of Michelson contrasts (Michelson, 1927) and temporal frequencies. Spatial frequency was held at 0.056 cycles per degree as this had previously been found to be the optimal spatial frequency to measure SSVEP recordings from Drosophila (West et al., 2015a). Stimuli were generated using the Psychophysics Toolbox on a Windows 7 PC and were displayed on dual 144Hz LCD monitors (XL240T, BenQ, Tiwam). Stimuli swept through unique combinations of 8 levels of temporal frequency (1, 2, 4, 6, 8, 12, 18 and 36 Hz) and 8 levels of contrast (1, 4, 8, 16, 32, 64, 99%) to generate 64 different combinations of temporal contrast stimuli. Parameter combinations were presented in a random order for an 11 second trial, with a 4 second inter-stimulus interval. The first second of each trial was removed prior to analysis to remove onset transients. Each parameter combination was presented 3 times per fly to create a ~1-hour recording session.

Analysis

Steady state visually evoked potentials

The periodic modulation of a contrast reversing grating evokes steady-state, visually evoked potentials (SSVEPs) with a phase-locked, periodic time course which is analysed most conveniently in the frequency domain (see Figure 1A and C for examples of SSVEP response from w^{-} and PINK1 mutants). For a single contrast

reversing grating, the ERG records responses from both the photoreceptors and the subsequent neuronal signalling pathways (Afsari et al., 2014). Individual photoreceptors will track the luminance modulations of the grating bars at the input frequency (F1) but because the signal elicited by a grating is a population average of photoreceptors driven by different transition polarities (some dark->light, some light->dark) the overall photoreceptor contribution is largely self-cancelling. Residual responses at F1 arise from asymmetries in photoreceptor sampling of the relatively low spatial frequency grating. The majority of the signal is composed of the transient responses arising from the visual neurons which are confined to even multiples of the input frequency. Of these responses, the second harmonic is by far the largest and we restrict our analyses to 2f for each input frequency. A coherently averaged (phase-sensitive) Fourier amplitude was calculated for each temporal frequency and contrast combination by averaging complex frequency-domain data obtained for each condition over 3 runs (see Figure 1B and D for examples of Fourier amplitudes from w^{-} and PINK1 mutants). Due to the phase-locked nature of VEPs, coherent averaging preserves the signal while phase-randomized noise sums to zero (Norcia et al., 2015).This results in a high signal to noise ratio for SSVEP recordings.

FIGURE 1 HERE

Linear discriminant analysis

We assessed LDA as a tool to accurately assign flies into their correct genotype based on multivariate visual response profiles. We used ERG measurements recorded in response to 64 combinations of contrast and temporal frequency, thus, providing a 64-dimensional dataset to input into the LDA. Each fly was therefore located in a 64-dimensional space. Flies that showed similar

responses to these combinations of contrast and temporal frequency clustered together in this space. Thus, if different classes showed different visual responses, unique clusters for each class would form in this 64-dimensional space. The LDA algorithm then attempted to identify a single linear boundary between these clusters and classified each fly into a genotypic class by asking which side of this linear boundary the fly was situated. The accuracy of the LDA algorithm depends on the degree of separation between the genotypic clusters in the multidimensional feature space. This is further expanded upon in Figure 2, where we illustrate the process of raw data collection through to a range of possible classifications.

FIGURE 2 HERE

Results

Early-onset PD temporal contrast profile amplitudes are larger than controls

A series of exemplar raw SSVEP responses from both w^{-} and PINK1 mutants at different ages and stimulus contrasts are illustrated in Figure 3. Average Fourier amplitudes at 2f for each temporal contrast combination for each genotype are illustrated in Figure 4. Higher peak response amplitudes are represented by lighter colours whilst lower amplitudes are represented by darker colours. Visual response changes as a function of both contrast and temporal frequency, with responses in both wild-type and EOPD models peaking at high contrast (99%) and an intermediate temporal frequency (6-8Hz).

FIGURE 3 HERE

FIGURE 4 HERE

Principal Components Analysis

We computed a Principal Components Analysis (PCA) on the full dataset (N=250) (See Figure 5). This allowed us to retain just those principal components (PCs) that explain significant amounts of the overall variance, simplifying our 64-dimensional data significantly (Jolliffe & Cadima, 2016; West et al., 2015a). Our first PC explained 89.9% of total variance within the dataset and the univariate analysis that follows is based on the amplitude of this component while the multivariate analysis later in the paper is performed on the full dataset.

FIGURE 5 HERE

Main effects

A 5x5 between groups ANOVA was performed on the first principal component score (representing SSVEP amplitude) to assess if there was a difference in SSVEP amplitudes between Drosophila genotypes or ages. The analysis found a significant main effect of genotype**,** $F(4,225) = 21.428$, $p < .001$, indicating a difference in response amplitude between the five genotypes, when collapsed over age**.** The analysis also found a significant main effect of age $F(4,225) = 5,558$, $p < .001$**,** indicating a difference in response amplitude between the 5 ages, when collapsed over genotype. Finally, there was a significant interaction effect $F(16,225) = 2.984$, $p < .001$, indicating that response amplitude differed between genotype depending on age. A simple effects analysis was performed to tease out differences in our conditions and explore our interaction effect.

Simple effects analysis comparing between genotypes within each age group

A simple effects analysis was undertaken to explore differences in the SSVEP amplitudes of Drosophila genotypes within each age group, with Sidak corrections applied to all possible comparisons. The SSVEP amplitudes of each genotype as a function of age are illustrated in Figure 6, whilst all corresponding p values are presented in Statistical Supplements Tables 1-10. Analysis revealed that at 1 day of age, all EOPD mutations (i.e. excluding dLRRK^{ex1}) had significantly higher SSVEP amplitudes when compared to w^{-} control flies, ($p < .01$)**.** When comparing between 1 day old PD mutants, PINK1^{5} produced significantly higher SSVEP amplitudes when compared to both DJ-1$\alpha^{\Delta 72}$ ($p < .05$) and dLRRK^{ex1} mutants ($p < .01$). There were no other significant differences in the SSVEP amplitudes of PD mutants. The larger amplitudes of EOPD mutants did not hold over later ages as wild type response increased at 7 days of age (see Figure 6). However, differences between the SSVEP amplitudes of PD mutants was found at these later ages. At 7 days of age PINK1^{5} mutants produced significantly higher amplitudes when compared to dLRRK^{ex1} ($p < .005$), whilst at 14 days of age DJ1-$\beta^{\Delta 93}$ had significantly higher amplitudes when compared to DJ-1$\alpha^{\Delta 72}$ ($p < .001$) and dLRRK^{ex1} ($p < .001$) mutants. This trend continued at 21 days of age, with DJ1-$\beta^{\Delta 93}$ continuing to show higher SSVEP amplitudes when compared to DJ-1$\alpha^{\Delta 72}$ ($p < .01$) and dLRRK^{ex1} ($p < .05$). At 28 days of age, DJ1-$\beta^{\Delta 93}$ ($p < .01$) and PINK1^{5} ($p = .01$) produced significantly higher SSVEP amplitudes when compared to DJ-1$\alpha^{\Delta 72}$.

FIGURE 6 HERE

Simple effects analysis comparing between age group within each genotype

A simple main effects analysis was undertaken to explore differences in the SSVEP amplitudes within each Drosophila genotype over its lifespan, with Sidak corrections applied to all possible comparisons. The p values for all simple effects are presented in Supplements. Analysis revealed that w^{-} response amplitudes increased between 1 and 7 days of age ($p = .001$), however there was no significant difference when comparing between further consecutive ages within this genotype, thus, visual response held stable between 7 to 28 days of age. There was a significant increase in DJ1-$\beta^{\Delta 93}$ response amplitudes between 7 and 14 days of age ($p < .001$), which then held steady from 14 to 28 days of age. There was no significant difference in response amplitudes within DJ-1$\alpha^{\Delta 72}$, PINK1^{5} or dLRRK^{ex1} at any consecutive ages between 1 and 28 days.

Increased demand for energy in the visual system leads to loss of visual response in old PD flies

While we demonstrated that abnormal gain control occurs in 1 day old EOPD mutants, at later ages, responses were comparable to those of wild-type flies (w^{-}). This represents a difference between EOPD mutant flies and flies mimicking the late-onset LRRK2-G2019S mutation, where responses fall to zero at later ages (Hindle et al., 2013). We hypothesized that maintaining our Drosophila stocks at 25° and a 12:12 LD cycle did not produce enough neuronal demand on the visual system to see any effect. To test this hypothesis, we increase the demand for energy by exposing Drosophila to irregular ~1.5s flashes of light of at random periodic intervals over seven days. Here, we hypothesise that the abnormal gain we have observed in young EOPD flies will interact with a visually induced increase in neural demand to cause an excitotoxic cascade.

Observation of temporal contrast response profiles (see Figure 7) indicated a profound reduction in SSVEP amplitudes across temporal frequency and contrast combinations for PD mutants (but not wild-type flies) after seven days exposure to photic stress.

FIGURE 7 HERE

A one way between groups ANOVA was performed on the first principal component score (representing SSVEP amplitude) extracted via the PCA analysis to assess if there was a significant difference in visual response between five Drosophila genotypes after they had been exposed to seven days of photic stress. The analysis found a significant main effect of genotype, $F(1,43) = 5.965$, $p = .001$, $\eta^2 = .357$, indicating a difference in response amplitude between the five genotypes. Pairwise comparisons revealed that all PD mutants produced significantly lower SSVEP amplitudes when compared to w^- control flies ($p < .05$), indicating an interaction between visual stimulation and Drosophila genotype on visual response amplitudes (see Figure 8). There was no significant difference between the PD mutants' SSVEP responses.

FIGURE 8 HERE

Linear discriminant analysis classifies flies into their correct genotypic class

Thus, all EOPD mutants show both an early increased visual response and a loss of vision after 7 days of visual stimulation, compared to w^- control flies.

In the presentation of our data so far, we utilized PCA to reduce the dimensionality in our data to a single variable, thereby removing any nuanced differences between full Drosophila temporal contrast profiles. We now explore how linear discriminant analysis can use the additional small, but significant sources of variation in our SSVEP data to classify Drosophila into their correct genotypic class and age group.

Linear Discriminant Analysis (LDA) is a statistical method that aims to answer both binary and multi-class classification problems by seeking linear combinations of variables that best explain the variance within the data, working under the assumption that unique classes generate unique Gaussian distributions (Izenman, 2008). We assess the accuracy of our LDA in two ways. First, we use a standard linear classifier (Fisher, 1936) as implemented in MATLAB's (2017a, Mathworks, MA) 'classify' function to conduct a leave one out (LOO) analysis, where the classifier receives training data from all flies to be assessed except one, then we measure the classifiers accuracy in classifying the excluded fly. This fly is resubstituted and the classification is repeated for every fly in the dataset to return a generalized LOO accuracy. Second, use MATLAB's classification function 'fitcdiscr' to fit an LDA model to our raw 64-dimensional data. We then use Monte Carlo resampling methods to produce 3 estimates of accuracy – an overall model accuracy, an N-way classification accuracy (the accuracy of correctly classifying a fly into one of the 5 genotypes at each age group or 5 age groups for each genotype) and a pair-wise classification accuracy (the accuracy of correctly classifying a fly into one of two correct genotypes at each age group). For detailed description of the

methods we used to apply LDA to multivariate Drosophila data, please see West et al. (2015).

Here, we hypothesise that Drosophila will be classified into their correct genotypic class at above-chance levels based on temporal contrast profiles, in line with previous findings using spatiotemporal profiles (West et al., 2015a).

Overall Model Discrimination Accuracy

We first ran our full dataset of 25 classes through the LDA to assess how well it could classify Drosophila when considering both their genotype and age. In this case, baseline (chance) performance was 4% (1/25). Next, to assess how well we could discriminate between Drosophila genotypes within each age group, our data were partitioned into 5 genotypes and LDA was applied with a 20% chance baseline (1/5). Finally, to assess how well we could classify between Drosophila at different ages within each genotype, our data were divided into 5 age groups within each genotype and analysed using LDA, again with a 20% chance baseline (1/5).

The full overall classification accuracies for both LOO analysis and Monte Carlo resampling analysis for all 3 sets of data are presented in Table 11. The overall accuracy of our model in classifying Drosophila into their correct genotypic class differed depending on the age of the genotypes included in the model. The highest classifications occurred at 1 and 28 days of age. Although there was a slight decrease in accuracies when classifying Drosophila into their correct age within a genotype, the algorithm still performed above 20% chance baseline for all genotypes.

Class	LOO Classification	Monte Carlo Resampling
All 25 classes	24.8%	29.6%
1 day post eclosion	58%	68%
7 days post eclosion	52%	64%
14 days post eclosion	46%	54%
21 days post eclosion	48%	50%
28 days post eclosion	64%	70%
w^{-}	54%	54%
DJ-1$\alpha^{\Delta 72}$	38%	38%
DJ1-$\beta^{\Delta 93}$	52%	52%
PINK1^{5}	34%	50%
dLRRK^{ex1}	26%	34%

Table 11: Classification accuracy differs when flies are grouped by age and classified into genotype, and when they are grouped by genotype and classified into age. Generally, both LOO and Monte Carlo resampling methods provide similar classification accuracies. N=50 for per class (chance baseline 20%), except 'All 25 classes' N=250 (chance baseline 4%).

N-Way Classification Accuracy

The confusion matrix was used to establish the accuracy of our LDA model to classify Drosophila into their correct genotypic class. Again, we investigated the precision of our model when all 25 classes were included in the model, with a 4% chance baseline (1/25). All classifications were reported above chance, bar PINK1^{5} at 21 days of age. The highest accuracy was for w^{-} at 1 day of age, where the

model performed with 34.49% accuracy, whilst most other conditions were classified with ~25% accuracy. A profile of classification accuracies when all 25 classes are considered is presented in Figure 9.

FIGURE 9 HERE

Next, we assessed the ability of the classifier to accurately genotype Drosophila within each age group, thus, five genotypes at each age were included in the model, with a 20% chance baseline (1/5). Our classification accuracy is deduced by normalizing our confusion matrix by dividing by the number of flies in each condition (n=10). As illustrated in Figure 10, at 1 day of age our model could classify w^{-} control flies into their correct genotypic class with 78.8% accuracy, whilst we could classify DJ-1$\alpha^{\Delta 72}$ at 45.5% accuracy, DJ1-$\beta^{\Delta 93}$ at 52.9% accuracy, PINK1^{5} at 73.6% accuracy and dLRRK^{ex1} at 60.0% accuracy.

FIGURE 10 HERE

These accuracies shifted at seven days of age, with our model classifying w^{-} with 29.8% accuracy, DJ-1$\alpha^{\Delta 72}$ with 50.0% accuracy, DJ1-$\beta^{\Delta 93}$ with 64.7% accuracy, PINK1^{5} with 62.2% accuracy and dLRRK^{ex1} at 46.9% accuracy. At 14 days of age our model could accuracy classify w^{-} at 50.0% accuracy, DJ-1$\alpha^{\Delta 72}$ at 68.1% accuracy, DJ1-$\beta^{\Delta 93}$ at 50.3% accuracy, PINK1^{5} at 36.4% accuracy and dLRRK^{ex1} at 29.1% accuracy. At 21 days of age with our model classified w^{-} at 58.35% accuracy, DJ-1$\alpha^{\Delta 72}$ at 50.5% accuracy, DJ1-$\beta^{\Delta 93}$ at 50.2% accuracy, PINK1^{5} at 25.7% accuracy and dLRRK^{ex1} 53.8% accuracy**.** At 28 days of age our

model classified w^{-} with 53.7% accuracy, DJ-1$\alpha^{\Delta 72}$ with 71.5% accuracy, DJ1-$\beta^{\Delta 93}$ with 62.6% accuracy, PINK1^{5} with 55.1% accuracy and dLRRK^{ex1} at 46.35% accuracy.

N-Way Classification Accuracy: Age

Here, our LDA model was used to classify Drosophila mutants into their correct age within a single genotype, with a 20% chance baseline (1/5). Comparatively, the model was generally weaker in accurately classifying into age when compared to classifying into genotype, although all classifications exceeded chance baseline. Age N-Way classification accuracies for each genotype are presented in Table 12.

	N-Way Classification Accuracy				
Genotype	1 day	7 days	14 days	21 days	28 days
w^{-}	81.3%	29.5%	32%	53.5%	53.5%
DJ-1$\alpha^{\Delta 72}$	26.6%	34.1%	50.0%	29.7%	48.4%
DJ1-$\beta^{\Delta 93}$	55.3%	59.5%	51.0%	45.0%	57.3%
PINK1^{5}	39.7%	49.1%	35.0%	27.2%	49.3%
dLRRK^{ex1}	37.6%	23.7%	22.7%	30.2%	43.7%

Chance baseline: 20% (1/5)

Table 12: N-Way classification of flies into their correct age differs between genotypes. All classes can be classified above 20% chance baseline, with the highest accuracy sitting at 81.3% for 1 day old w^{-} classifications. n=10

Pairwise Classification Accuracy

To assess the accuracy of our model in classifying Drosophila between pairs of genotypes within each age group we bootstrapped our data through 1000 iterations of a two-way classification analysis. Here, we assess the accuracy of the algorithm estimation in classifying a fly from a pair of genotypes into its correct class. Classification is significantly above chance when fewer than 5% of the bootstrapped 2-way classification probabilities are .5 or greater.

As presented in Table 13, the algorithm classified one-day old Drosophila genotypes with accuracy between 73.7% - 94.1% ($p<.05$). Notably, all PD mutants could be accurately distinguished from w^{-} control flies.

	w^{-}	DJ1-$\beta^{\Delta 93}$	DJ-1$\alpha^{\Delta 72}$	dLRRK^{ex1}
PINK1^{5}	94.1%*	84.7%*	78.8%*	88.9%*
w^{-}	-	86.3%*	75.8%*	77.6%*
DJ1-$\beta^{\Delta 93}$	-	-	57.9%	73.7%*
DJ-1$\alpha^{\Delta 72}$	-	-	-	65.3%

* = $p < .05$

Table 13: LDA can accurately compute pairwise classifications between PD and control genotypes at 1 day of age (n=10).

As presented in Table 14, at 7 days of age the model had a reduction in the amount of significant comparisons, performing between 74.5% - 85.6% accuracy. At this age, the LDA could not accurately discriminate between any of the PD mutants and control flies.

	w^{-}	DJ1-$\beta^{\Delta 93}$	DJ-1$\alpha^{\Delta 72}$	dLRRK^{ex1}
PINK1^{5}	69.9%	74.7%*	76.1%*	85.6%*
w^{-}	-	60.8%	60.5%	63.3%
DJ1-$\beta^{\Delta 93}$	-	-	67.7%	76.3%*
DJ-1$\alpha^{\Delta 72}$	-	-	-	66.9%

* = p < .05

Table 14: LDA had a reduction in total significant comparisons at 7 days of age, and cannot accurately discriminate between any of the PD mutants when compared against control flies (n=10).

At 14 days of age there appeared to be an overall improvement in pairwise classifications with significant pairwise classifications between 78.0% - 81.3% accuracy, as illustrated in Table 15.

	w^{-}	DJ1-$\beta^{\Delta 93}$	DJ-1$\alpha^{\Delta 72}$	dLRRK^{ex1}
PINK1^{5}	61.7%	57.8%	78.6%*	79.2%*
w^{-}	-	78.4%*	78.0%*	79.9%*
DJ1-$\beta^{\Delta 93}$	-	-	89.6%*	91.3%*
DJ-1$\alpha^{\Delta 72}$	-	-	-	52.1%

* = p < .05

Table 15. LDA can accurately compute pairwise classifications between PD and control genotypes at 14 days of age (n=10). There are differences in accuracy when compared to 7 and 1 day old classifications.

This held at 21 days of age, where our pairwise classification accuracy reached between 75.2% - 85.1% for significant comparisons, as illustrated in Table 16, however there was a reduction in significant comparisons at this age.

	w^{-}	DJ1-$\beta^{\Delta 93}$	DJ-1$\alpha^{\Delta 72}$	dLRRK^{ex1}
PINK1^{5}	63.3%	65.2%	75.2%*	52.9%
w^{-}	-	78.4%*	77.4%*	69.4%
DJ1-$\beta^{\Delta 93}$	-	-	85.1%*	77.7%*
DJ-1$\alpha^{\Delta 72}$	-	-	-	60.6%

* = p < .05

Table 16. LDA can accurately compute pairwise classifications between PD and control genotypes at 21 day of age (n=10), however there are less significant comparisons compared to earlier ages.

In line with our peak in overall model accuracy, our model was most accurate in classifying between flies at 28 days of age, with all possible comparisons statistically significant and sitting between 72.7% and 86.2% accuracy (Table 17). Similar to one day old comparisons, all PD mutants could be accurately distinguished from w^{-} control flies at 28 days of age. We note that these statistics differ from the comparisons on the PCA simple effects analysis data, as will be addressed in our discussion.

	w^{-}	DJ1-$\beta^{\Delta 93}$	DJ-1$\alpha^{\Delta 72}$	dLRRK^{ex1}
PINK1^{5}	78.9%*	78.7%*	79.7%*	73.7%*
w^{-}	-	86.2%*	81.0%*	75.6%*
DJ1-$\beta^{\Delta 93}$	-	-	88.4%*	83.6%*
DJ-1$\alpha^{\Delta 72}$	-	-	-	72.7%*

* = $p < .05$

Table 17. LDA accurately computes pairwise classifications between all genotypes at 28 days of age (n=10). All comparisons are significant and above 72.7% accuracy.

Discussion

Abnormal gain control in early-onset PD Drosophila models

We have demonstrated that abnormal gain control occurs in young EOPD mutants; DJ-1$\alpha^{\Delta 72}$, DJ1-$\beta^{\Delta 93}$, and PINK1^{5}. Drosophila with these mutations have significantly higher SSVEP response amplitudes when compared to w^{-} controls at day 1. Notably, there appears to be no difference between response amplitudes of 1 day old w^{-} controls and knockout of the fly LRRK2 homologue dLRRK^{ex1}. These results are consistent with previous studies, and point to a common phenotype of abnormal gain control occurring in the current studied EOPD mutants and the LRRK2-G2019S late-onset mutant (Afsari et al., 2014; West et al., 2015a).

What common biological mechanism might explain these findings? Dopaminergic terminals are found in the Drosophila ommatidium, lamina, and medulla, where dopamine is thought to regulate contrast sensitivity, light adaptation, and circadian rhythms (Afsari et al., 2014; Chyb et al., 1999; Hirsh et al., 2010; Jackson et al., 2012; Nassel & Elekes, 1992). Thus, dopamine acts as a

554 neuromodulator within the Drosophila visual system, effectively regulating neural
555 response to visual excitation. PD-model flies may have less dopamine content,
556 and/or fewer dopaminergic neurons, or disrupted dopamine signalling, though the
557 reduction may depend on the environmental conditions (Navarro et al., 2014; Ng et
558 al., 2012; Park et al., 2006; Wang et al., 2006). Any reduction in dopamine release
559 will cause photoreceptors to respond faster and with greater amplitude (Chyb et al.,
560 1999). This hyperactivity causes increased SSVEP amplitudes, manifesting as
561 abnormal gain control. Humans, like flies, have retinal dopamine within the amacrine
562 cells and inner border of the nuclear layer, where it is thought to be responsible for
563 light adaptation, contour perception, and contrast sensitivity (Crooks & Kolb, 1992;
564 Dowling, 1979; Witkovsky, 2004). Human patients also show a reduction in retinal
565 dopamine and report a range of low-level visual deficits, including poor contrast
566 sensitivity and reduced light sensitivity (Archibald, Clarke, Mosimann, & Burn, 2011;
567 Beitz, 2014; Chaudhuri & Schapira, 2009; Weil et al., 2016). These homologies in
568 retinal structure, function, and disease pathology point to the possibility that
569 prodromal gain control abnormalities occur in human PD patients.
570
571 The response profile of wild-type w^{-} Drosophila changes as a function of age.
572 This genotype initially presented with comparatively low response amplitudes when
573 compared to EOPD mutants. w^{-} response then increased between 1 and 7 days of
574 age. This reflects the anatomical plasticity of the young Drosophila visual system.
575 Young w^{-} flies are born with reduced visual sensitivity which then adapts to
576 functional requirements, with visual maturity occurring between 4 - 7 days of age
577 (Kral & Meinertzhagen, 1989). It is important to note that all Drosophila included in
578 our study are white eyed, thus share the w^{-} mutation. The increased sensitivity to

visual stimuli we observe in EOPD mutants, and mutants' unique developmental profiles, is due solely to the PD mutation.

Excitotoxicity as a pathol*ogical phenotype in Parkinson's d*isease

Initially we saw no evidence of excitotoxic damage in the visual system of older PD flies. However, Drosophila in the lab experience a relatively stable visual environment: light levels are many orders of magnitude lower than those in the outside world and they are modulated according to a strict 12hr:12hr LD cycle. We theorised that purposeful visual stimulation of the PD Drosophila visual system may be necessary to induce excitotoxicity in the lab. To increase neural demand for energy we exposed flies to a rich visual environment which contained irregular bursts of high intensity luminance modulations. This environment requires the photoreceptors both to change their firing rates and their mean sensitivity over relatively short time periods. Our hypothesis was that the abnormal gain control we observed in young EOPD flies would interact with an increase in neural activity to cause an excitotoxic cascade. Our data are consistent with this hypothesis – PD, but not w^{-} flies, showed reduced visual functionality after prolonged exposure to these visually demanding environments.

Our results provide evidence for an excitotoxic cascade in PD Drosophila mutants, with DJ-1$\alpha^{\Delta 72}$, DJ1-$\beta^{\Delta 93}$, and PINK1^{5} all showing a significant decrease in SSVEP amplitudes after seven days of visual stimulation, with a minimum of 50% reduction in response. Surprisingly, the response amplitudes of dLRRK^{ex1} mutants were also reduced, even though we did not observe abnormal gain control in this strain at one day of age.

We draw upon the previously established theory of excitotoxicity in PD explain the biological processes underlying our observed visual loss. Here, abnormal gain control interacts with a visually induced increase in neural demand. This causes an increase in ionic flux across the cell membrane which in turn results in extra demand for ATP from the ion exchange pumps. When mitochondria cannot meet this increased demand for ATP, they release reactive oxygen species (e.g. superoxide, hydrogen peroxide), so generating oxidative stress, which leads to autophagy, apoptosis and other forms of cell damage. This is then followed visual decline and eventual cell death (Hindle et al., 2013).

Mitochondrial dysfunction and oxidative stress appear to play a central role in PD pathogenesis (Bogaerts, Theuns, & Van Broeckhoven, 2008; Büeler, 2009; Henchcliffe & Beal, 2008; Schapira, 2008). The current paper has investigated Drosophila PD mutations in genes whose human homologues are associated with EOPD. In both humans and flies, DJ-1 encodes a small protein that is thought to protect against oxidative stress and assist in mitochondrial regulation by acting as a sensor for Reactive Oxidative Species (ROS) (Oswald et al., 2016). Subsequently, loss-of-function mutations in DJ-1 appear to increase cell death in response to oxidative stress. Further, animal studies have observed perturbations in dopamine release in DJ-1 deficient animal models, although there is no physiological loss of dopamine neurons (Goldberg et al., 2005; Martella et al., 2011; Menzies, Yenisetti, & Min, 2005; Meulener et al., 2005; Pisani et al., 2006; Yang, Chen, Ding, Zhuang, & Kang, 2007). PINK1 is a protein kinase with a mitochondrial targeting sequence and acts to maintain mitochondrial homeostasis in dopaminergic neurons (Park et al.,

2006). Likewise, studies in PINK1 animal models have found evidence for abnormal mitochondrial morphology and impaired dopamine release (Clark et al., 2006; Kitada et al., 2007; Park et al., 2006)**.** Thus, the protein products of both DJ-1 and PINK1 both play roles in the regulation of cellular energy production. However, loss-of-function mutations on these genes negatively impact mitochondria in different ways. Our data provide additional support for the hypothesis that mitochondrial impairment plays a role in the pathogenesis of genetic PD.

Classification of Drosophila PD genotype

Previously, we demonstrated that discriminant analysis is a useful tool that can accurately classify PD Drosophila into their correct genotypic class at 1 day of age (West et al., 2015a). Here, we build upon this observation, establishing that variability within temporal contrast response profiles obtained from Drosophila can be used in a LDA to accurately classify Drosophila into their correct genotypic class at various ages with above chance accuracy. When all 25 classes were included in our model, our LOO classification accuracy sat at 24.8%, whilst our bootstrapped classification accuracy was 29.6% (chance baseline of 4%). Our LDA model also performed well when classifying five genotypes within a single age group. Highest classifications occurred at one day (Monte Carlo sampling accuracy of 68% and LLO accuracy of 58%) and 28 days of age (Monte Carlo sampling accuracy of 70% and LOO accuracy of 64%) with a baseline of 20%. This indicates that there are substantial differences between Drosophila genotypes at both one and 28 days of age.

When all 25 classes were included in our model, all classifications (except PINK1^{5}) perform above a 4% chance baseline, with most classifications occurring with ~25% accuracy. There is substantial variation between PD Drosophila visual response throughout their lifespan, indicating that EOPD mutations have unique effects on Drosophila visual pathways at not only one day of age, but throughout the Drosophila lifespan. After our data were partitioned into five genotypes for each age group, we could classify Drosophila into their correct genotypic class with 29.8% - 78.8% accuracy over all possible age groups, with no classifications falling under the statistical chance baseline of 20%. Our results illustrate that mutants can be accurately classified into their correct genotypic class beyond one day of age, indicating there are subtle differences in how EOPD mutations affect Drosophila neural gain control, as will be discussed.

Although the N-Way classification accuracy decreased when the algorithm was required to classify Drosophila into their correct age within a single genotype, our model still performed above chance baseline. This is surprising considering the results of our first experiment, where, for the most part, within genotype responses did not significantly differ over time. Our analysis was run on a reduced number of genotypes and flies (n=10 and five genotypes, rather than n=20 and 10 genotypes as per West et al. (2015)), yet our model produced a consistently high classification accuracy, even with all 25 classes were included in the model. In West et al., (2015), we varied temporal and spatial frequency but kept contrast fixed. We observed relatively little dependence on spatial frequency up to a hard cut-off that was associated with spatial sampling limits. Our use of contrast rather than spatial frequency in the experiments described here allows us to measure the full contrast

678 sensitivity profile of each genotype and age, increasing the sensitivity of this
679 multivariate visual biomarker for EOPD genes in Drosophila. Further, our assay,
680 when combined with LDA, is sensitive enough to detect small differences in the
681 effect of EOPD mutations on Drosophila neural gain control. Our initial analysis
682 found a substantial difference between w^{-} and EOPD mutants at 1 day of age,
683 however our LDA results indicate that these mutations have their own subtle effects
684 on neural gain control across Drosophila lifespan. Our findings carry an important
685 implication. As noted, DJ-1 acts as a ROS sensor, whilst PINK1 acts to maintain
686 mitochondrial homeostasis in dopaminergic neurons (Lavara-Culebras, Muñoz-
687 Soriano, Gómez-Pastor, Matallana, & Paricio, 2010; Oswald et al., 2016; Park et al.,
688 2006). The ability of our LDA to accurately distinguish between mutations on these
689 genes indicates each mutation uniquely impacts the underlying cellular processes
690 thereby causing a subtle, dissimilar neural responses across Drosophila lifespan,
691 that then results in a common pathogenic outcome of visual loss and cell death.
692
693 A key benefit of using Drosophila as disease model is their convenience for
694 early-stage drug testing due to their fecundity and fast generation time. It is
695 advantageous to have phenotypic expression of PD mutations at early stages of
696 Drosophila lifespan as this supports their utility as an initial model for the rapid
697 testing of neuroactive drugs that have the potential to treat human disease. Like
698 Drosophila, perturbations in contrast sensitivity occur in human PD patients due to
699 reduced dopamine levels within the retina (Harnois & Di Paolo, 1990). Our current
700 findings may correspond to the changes seen in human PD patients, although there
701 is obvious difficulty in assessing whether a prodromal abnormal gain control occurs
702 in the early stages of pre-genotyped PD patients. We believe that it may be possible

for LDA to classify human PD patients genotype based on multivariate SSVEP response profiles as measured by electroencephalogram (EEG). This would have the potential to assist in early PD diagnosis, genotypic classification, and disease expression. Our next step is to investigate Drosophila response to additional low level visual parameters such as chromatic contrast and orientation, and deduce whether a similar biomarker can be established in human PD patients.

Together, our experiments have uncovered abnormal gain control and an excitotoxic cascade as a common pathological phenotype in three EOPD mutations, DJ-1$\alpha^{\Delta 72}$, DJ1-$\beta^{\Delta 93}$, and PINK1[5]. In addition to furthering the link between abnormal gain control and excitotoxicity in genetic forms of PD, our findings have built upon the utility of LDA in genotyping Drosophila based on multivariate response profiles. Further, we have illustrated that there are variations in how these EOPD mutations affect neural gain control across Drosophila lifespan, indicating that these mutations have unique effects upon underlying cellular processes that lead to a common outcome – visual loss and cell death. Overall, it appears that these PD related mutations are heterochronic: in young flies, mutations lead to stronger neural signalling (increased sensory response may be beneficial in escaping behaviour) but are detrimental in older flies (a loss of vision would hinder escape behaviour) (Himmelberg, West, Wade, & Elliott, 2017). Should these findings in fly models prove applicable to the human situation, it would suggest that prodromal PD may be linked to changes in central nervous system processing that could, potentially, confer advantages in early life at the cost of degenerative disease in old age.

Acknowledgments: We would like to thank Dr Sean Sweeny and Dr Alex Whitworth who generously donated fly stocks used in the study.

Grants: M.M.H was supported by the European Union's Horizon 2020 research and innovation programme under the Marie Sklodowska-Curie grant agreement No 641805. R.J.H.W developed the original equipment and methods under support from the Wellcome Trust and the York Centre for Chronic Diseases and Disorders (C2D2).

Disclosures: No conflicts of interest, financial or otherwise, are declared by the authors.

Author Contributions: Data were collected by M.M.H. All authors contributed to the design, implementation and analysis as well as writing the paper.

References

Afsari, F., Christensen, K. V., Smith, G. P., Hentzer, M., Nippe, O. M., Elliott, C. J. H., & Wade, A. R. (2014). Abnormal visual gain control in a Parkinson's disease model. Human Molecular Genetics, 23(17), 12. https://doi.org/10.1038/nrn2619

Archibald, N. K., Clarke, M. P., Mosimann, U. P., & Burn, D. J. (2011). Visual symptoms in Parkinson's disease and Parkinson's disease dementia. Movement Disorders, 26(13), 2387–2395. https://doi.org/10.1002/mds.23891

Beal, M. F., Brouillet, E., Jenkins, B. G., Ferrante, R. J., Kowall, N. W., Miller, J. M., … Hyman, B. T. (1993). Neurochemical and histologic characterization of striatal excitotoxic lesions produced by the mitochondrial toxin 3-nitropropionic acid. *The Journal of Neuroscience : The Official Journal of the Society for* Neuroscience, 13(October), 4181–4192.

Beitz, J. M. (2014). Parkinson's disease: a review. Frontiers in Bioscience (Scholar Edition), 6, 65–74. https://doi.org/10.2741/S415

Bogaerts, V., Theuns, J., & Van Broeckhoven, C. (2008). Genetic findings in Parkinson's disease and translation into treatment: A leading role for mitochondria? Genes, Brain and Behavior. https://doi.org/10.1111/j.1601-183X.2007.00342.x

Büeler, H. (2009). Impaired mitochondrial dynamics and function in the pathogenesis of Parkinson's disease. Experimental Neurology. https://doi.org/10.1016/j.expneurol.2009.03.006

Busse, L., Wade, A. R., & Carandini, M. (2009). Representation of Concurrent Stimuli by Population Activity in Visual Cortex. Neuron, 64(6), 931–942. https://doi.org/10.1016/j.neuron.2009.11.004

Carandini, M., & Heeger, D. (1994). Summation and division by neurons in primate

visual cortex. Science (New York, N.Y.), 264(5163), 1333–1336. https://doi.org/10.1126/science.8191289

Carandini, M., & Heeger, D. J. (2011). Normalization as a canonical neural computation. Nature Reviews Neuroscience. https://doi.org/10.1038/nrn3136

Carandini, M., Heeger, D. J., & Movshon, J. A. (1997). Linearity and normalization in simple cells of the macaque primary visual cortex. The Journal of *Neuroscience : The Official Journal of the Society for Neuroscience*, 17(21), 8621–8644.

Chaudhuri, K. R., & Schapira, A. H. (2009). Non-motor symptoms of Parkinson's disease: dopaminergic pathophysiology and treatment. The Lancet Neurology. https://doi.org/10.1016/S1474-4422(09)70068-7

Chyb, S., Hevers, W., Forte, M., Wolfgang, W. J., Selinger, Z., & Hardie, R. C. (1999). Modulation of the light response by cAMP in Drosophila photoreceptors. *The Journal of Neuroscience : The Official Journal of the Society for* Neuroscience, 19(20), 8799–8807.

Clark, I. E., Dodson, M. W., Jiang, C., Cao, J. H., Huh, J. R., Seol, J. H., … Guo, M. (2006). Drosophila pink1 is required for mitochondrial function and interacts genetically with parkin. Nature, 441(7097), 1162–6. https://doi.org/10.1038/nature04779

Clarke, C. E. (2007). Parkinson's disease. BMJ (Clinical Research Ed.), 335(7617), 441–5. https://doi.org/10.1136/bmj.39289.437454.AD

Crooks, J., & Kolb, H. (1992). Localization of GABA, glycine, glutamate and tyrosine hydroxylase in the human retina. Journal of Comparative Neurology, 315(3), 287–302. https://doi.org/10.1002/cne.903150305

de Rijk, M. C., Tzourio, C., Breteler, M. M., Dartigues, J. F., Amaducci, L., Lopez-

802 Pousa, S., … Rocca, W. A. (1997). Prevalence of parkinsonism and Parkinson's
803 disease in Europe: the EUROPARKINSON Collaborative Study. European
804 Community Concerted Action on the Epidemiology of Parkinson's disease.
805 Journal of Neurology, Neurosurgery, and Psychiatry, 62(1), 10–5.
806 https://doi.org/10.1136/jnnp.62.1.10
807 Dowling, J. E. (1979). A new retinal neurone - the interplexiform cell. Trends in
808 Neurosciences, 2(C), 189–191. https://doi.org/10.1016/0166-2236(79)90076-6
809 Fisher, R. A. (1936). The use of multiple measures in taxonomic problems. Annals of
810 Eugenics, 7(2), 179–188. https://doi.org/10.1111/j.1469-1809.1936.tb02137.x
811 Goldberg, M. S., Pisani, A., Haburcak, M., Vortherms, T. A., Kitada, T., Costa, C., …
812 Shen, J. (2005). Nigrostriatal dopaminergic deficits and hypokinesia caused by
813 inactivation of the familial parkinsonism-linked gene DJ-1. Neuron, 45(4), 489–
814 496. https://doi.org/10.1016/j.neuron.2005.01.041
815 Harnois, C., & Di Paolo, T. (1990). Decreased dopamine in the retinas of patients
816 with Parkinson's disease. Investigative Ophthalmology and Visual Science,
817 31(11), 2473–2475.
818 Henchcliffe, C., & Beal, M. F. (2008). Mitochondrial biology and oxidative stress in
819 Parkinson disease pathogenesis. Nature Clinical Practice. Neurology, 4(11),
820 600–609. https://doi.org/10.1038/ncpneuro0924
821 Himmelberg, M. M., West, R. J. H., Wade, A. R., & Elliott, C. J. H. (2017). A
822 perspective plus on Parkinson's disease. Movement Disorders.
823 Hindle, S., Afsari, F., Stark, M., Adam Middleton, C., Evans, G. J. O., Sweeney, S.
824 T., & Elliott, C. J. H. (2013). Dopaminergic expression of the Parkinsonian gene
825 LRRK2-G2019S leads to non-autonomous visual neurodegeneration,
826 accelerated by increased neural demands for energy. Human Molecular

827 Genetics, 22(11), 2129–2140. https://doi.org/10.1093/hmg/ddt061
828 Hirsh, J., Riemensperger, T., Coulom, H., Ich??, M., Coupar, J., & Birman, S. (2010).
829 Roles of Dopamine in Circadian Rhythmicity and Extreme Light Sensitivity of
830 Circadian Entrainment. Current Biology, 20(3), 209–214.
831 https://doi.org/10.1016/j.cub.2009.11.037
832 Izenman, A. J. (2008). Modern Multivariate Statistical Techniques. New York:
833 Springer-Verlag.
834 Jackson, C. R., Ruan, G.-X., Aseem, F., Abey, J., Gamble, K., Stanwood, G., …
835 McMahon, D. G. (2012). Retinal Dopamine Mediates Multiple Dimensions of
836 Light-Adapted Vision. Journal of Neuroscience, 32(27), 9359–9368.
837 https://doi.org/10.1523/JNEUROSCI.0711-12.2012
838 Jolliffe, I. T., & Cadima, J. (2016). Principal component analysis : a review and recent
839 developments Subject Areas : Author for correspondence :
840 Kitada, T., Pisani, A., Porter, D. R., Yamaguchi, H., Tscherter, A., Martella, G., …
841 Shen, J. (2007). Impaired dopamine release and synaptic plasticity in the
842 striatum of PINK1-deficient mice. Proc.Natl.Acad.Sci.U.S.A, 104(0027–8424
843 (Print)), 11441–11446. https://doi.org/10.1073/pnas.0702717104
844 Kral, K., & Meinertzhagen, I. a. (1989). Anatomical plasticity of synapses in the
845 lamina of the optic lobe of the fly. Philosophical Transactions of the Royal
846 Society of London. Series B, Biological Sciences, 323(1214), 155–183.
847 https://doi.org/10.1098/rstb.1989.0004
848 Lavara-Culebras, E., Muñoz-Soriano, V., Gómez-Pastor, R., Matallana, E., & Paricio,
849 N. (2010). Effects of pharmacological agents on the lifespan phenotype of
850 Drosophila DJ-1β mutants. Gene, 462(1–2), 26–33.
851 https://doi.org/10.1016/j.gene.2010.04.009

852 Longo, F., Russo, I., Shimshek, D. R., Greggio, E., & Morari, M. (2014). Genetic and
853 pharmacological evidence that G2019S LRRK2 confers a hyperkinetic
854 phenotype, resistant to motor decline associated with aging. Neurobiology of
855 Disease, 71, 62–73. https://doi.org/10.1016/j.nbd.2014.07.013
856 Martella, G., Madeo, G., Schirinzi, T., Tassone, A., Sciamanna, G., Spadoni, F., …
857 Bonsi, P. (2011). Altered profile and D2-dopamine receptor modulation of high
858 voltage-activated calcium current in striatal medium spiny neurons from animal
859 models of Parkinson's disease. Neuroscience, 177, 240–251.
860 https://doi.org/10.1016/j.neuroscience.2010.12.057
861 Matikainen-Ankney, B. A., Kezunovic, N., Mesias, R. E., Tian, Y., Williams, F. M.,
862 Huntley, G. W., & Benson, D. L. (2016). Altered Development of Synapse
863 Structure and Function in Striatum Caused by Parkinson's Disease-Linked
864 LRRK2-G2019S Mutation. *The Journal of Neuroscience : The Official Journal of*
865 the Society for Neuroscience, 36(27), 7128–41.
866 https://doi.org/10.1523/JNEUROSCI.3314-15.2016
867 Menzies, F. M., Yenisetti, S. C., & Min, K. T. (2005). Roles of Drosophila DJ-1 in
868 survival of dopaminergic neurons and oxidative stress. Current Biology, 15(17),
869 1578–1582. https://doi.org/10.1016/j.cub.2005.07.036
870 Meulener, M., Whitworth, A. J., Armstrong-Gold, C. E., Rizzu, P., Heutink, P., Wes,
871 P. D., … Bonini, N. M. (2005). Drosophila DJ-1 mutants are selectively sensitive
872 to environmental toxins associated with Parkinson's disease. Current Biology,
873 15(17), 1572–1577. https://doi.org/10.1016/j.cub.2005.07.064
874 Michelson, A. (1927). Studies in Optics. University of Chicago Press.
875 Mortiboys, H., Furmston, R., Bronstad, G., Aasly, J., Elliott, C., & Bandmann, O.
876 (2015). UDCA exerts beneficial effect on mitochondrial dysfunction in

LRRK2(G2019S) carriers and in vivo. Neurology, 85(10). https://doi.org/10.1212/WNL.0000000000001905.

Nassel, D. R., & Elekes, K. (1992). Aminergic neurons in the brain of blowflies and Drosophila: dopamine- and tyrosine hydroxylase-immunoreactive neurons and their relationship with putative histaminergic neurons. Cell Tissue Res., 267, 147–167.

Navarro, J. A., Heßner, S., Yenisetti, S. C., Bayersdorfer, F., Zhang, L., Voigt, A., … Botella, J. A. (2014). Analysis of dopaminergic neuronal dysfunction in genetic and toxin-induced models of Parkinson's disease in Drosophila. Journal of Neurochemistry, 131(3), 369–382. https://doi.org/10.1111/jnc.12818

Ng, C.-H., Guan, M. S. H., Koh, C., Ouyang, X., Yu, F., Tan, E.-K., … Lim, K.-L. (2012). AMP Kinase Activation Mitigates Dopaminergic Dysfunction and Mitochondrial Abnormalities in Drosophila Models of Parkinson's Disease. Journal of Neuroscience, 32(41), 14311–14317. https://doi.org/10.1523/JNEUROSCI.0499-12.2012

Norcia, A. M., Appelbaum, L. G., Ales, J. M., Cottereau, B. R., & Rossion, B. (2015). The steady-state visual evoked potential in vision research : A review. Journal of Vision, 15(6), 1–46. https://doi.org/10.1167/15.6.4.doi

Ogden, D. (1994). Microelectrode electronics. In D. Ogden (Ed.), Microelectrode Techniques. Cambridge: Company of Biologists.

Oswald, M. C. W., Brooks, P. S., Zwart, M. F., Mukherjee, A., Ryan, J. H., Morarach, K., … Landgraf, M. (2016). Reactive Oxygen Species Regulate Neuronal Structural Plasticity, 3. https://doi.org/http://dx.doi.org/10.1101/081968

Park, J., Lee, S. B., Lee, S. B., Kim, Y., Song, S., Kim, S., … Chung, J. K. (2006). Mitochondrial dysfunction in Drosophila PINK1 mutants is complemented by

parkin. Nature, 441(7097), 1157–1161. https://doi.org/10.1038/nature04788

Pisani, A., Martella, G., Tscherter, A., Costa, C., Mercuri, N. B., Bernardi, G., … Calabresi, P. (2006). Enhanced sensitivity of DJ-1-deficient dopaminergic neurons to energy metabolism impairment: Role of Na+/K+ ATPase. Neurobiology of Disease, 23(1), 54–60. https://doi.org/10.1016/j.nbd.2006.02.001

Ponzo, V., Di Lorenzo, F., Brusa, L., Schirinzi, T., Battistini, S., Ricci, C., … Koch, G. (2017). Reply Letter to “Does motor cortex plasticity depend on the type of mutation in the LRRK2 gene? Movement Disorders, 32(6), 949.

Regan, D. (1966). Some characteristics of average steady-state and transient respones evoked by modulated light. Electroencephalography and Clinical Neurophysiology, 20(3), 238–248.

Schapira, A. H. (2008). Mitochondria in the aetiology and pathogenesis of Parkinson’s disease. The Lancet Neurology. https://doi.org/10.1016/S1474-4422(07)70327-7

Single, S., Haag, J., & Borst, a. (1997). Dendritic computation of direction selectivity and gain control in visual interneurons. *The Journal of Neuroscience : The* Official Journal of the Society for Neuroscience, 17(16), 6023–6030.

Sloan, M., Alegre-Abarrategui, J., Potgieter, D., Kaufmann, A. K., Exley, R., Deltheil, T., … Wade-Martins, R. (2016). LRRK2 BAC transgenic rats develop progressive, L-DOPA-responsive motor impairment, and deficits in dopamine circuit function. Human Molecular Genetics, 25(5), 951–963. https://doi.org/10.1093/hmg/ddv628

Surmeier, D. J., Obeso, J. A., & Halliday, G. M. (2017). Parkinson’s Disease Is Not Simply a Prion Disorder. Journal of Neuroscience, 37(41).

https://doi.org/https://doi.org/10.1523/JNEUROSCI.1787-16.2017

Tyler, C. W., Apkarian, P., & Nakayama, K. (1978). Multiple spatial-frequency tuning of electrical responses from human visual cortex. Experimental Brain Research, 33(3–4), 535–550. https://doi.org/10.1007/BF00235573

Volta, M., Beccano-Kelly, D. A., Paschall, S. A., Cataldi, S., MacIsaac, S. E., Kuhlmann, N., … Milnerwood, A. J. (2017). Initial elevations in glutamate and dopamine neurotransmission decline with age, as does exploratory behavior, in LRRK2 G2019S mice. Elife, 20(6). https://doi.org/10.7554/eLife.28377

Wang, D., Qian, L., Xiong, H., Liu, J., Neckameyer, W. S., Oldham, S., … Zhang, Z. (2006). Antioxidants protect PINK1-dependent dopaminergic neurons in Drosophila. Proceedings of the National Academy of Sciences of the United States of America, 103(36), 13520–5. https://doi.org/10.1073/pnas.0604661103

Weil, R. S., Schrag, A. E., Warren, J. D., Crutch, S. J., Lees, A. J., & Morris, H. R. (2016). Visual dysfunction in Parkinson's disease. Brain, 139(11), 2827–2843. https://doi.org/10.1093/brain/aww175

West, R. J. H., Elliott, C. J. H., & Wade, A. R. (2015a). Classification of Parkinson's Disease Genotypes in Drosophila Using Spatiotemporal Profiling of Vision. Scientific Reports, 5(October), 16933. https://doi.org/10.1038/srep16933

West, R. J. H., Elliott, C. J. H., & Wade, A. R. (2015b). Classification of Parkinson's Disease Genotypes in Drosophila Using Spatiotemporal Profiling of Vision, 5, 16933. Retrieved from http://dx.doi.org/10.1038/srep16933

Witkovsky, P. (2004). Dopamine and retinal function. Documenta Ophthalmologica. https://doi.org/10.1023/B:DOOP.0000019487.88486.0a

Yang, W., Chen, L., Ding, Y., Zhuang, X., & Kang, U. J. (2007). Paraquat induces dopaminergic dysfunction and proteasome impairment in DJ-1-deficient mice.

Human Molecular Genetics, 16(23), 2900–2910.
https://doi.org/10.1093/hmg/ddm249

Figure Captions

Figure 1. Time-domain SSVEP with a stimulus input frequency of 8Hz contains 16 'reversals' / second and can be decomposed into a SSVEP response spectrum with peaks at multiples of the input frequency. In A) we present an averaged time-domain SSVEP response from a w^- fly to 99% contrast reversing sine grating over 1000ms, modulating at 8Hz, whilst B) shows Fourier amplitudes decomposed from Fourier transform the 8Hz waveform in A, with peaks occurring at multiples of our input frequency (8Hz, 16Hz, 24Hz, 32Hz, 40Hz). The same is shown in C) and D) for a $PINK1^5$ PD-mutant fly.

Figure 2. Analysis path for Linear Discriminant Analysis (LDA). The raw ERG (electroretinogram) response to 64 different stimuli is collected – here from a control (wild-type) w^- fly and an EOPD (PINK1) fly (A). For each stimulus, Fourier analysis is used to measure the response of the fly at the second harmonic (2f) (B). Each fly is exposed to 64 stimuli – each with a known contrast and temporal frequency. The heat map (C) represents the amplitude of the second harmonic at each stimulus condition. In this simple case, with just 2 genotypes at one time point, the LDA is applied to the data from both genotypes, and determines the equation that best separates the data into two classes based on the 64 responses. Three outcomes could be envisaged – an optimal separation of the data. Di) a clear line separates the data, or a partial separation (Dii), or no difference (Diii), all the data are mixed). In this portrayal, the graph plots 'X' and 'Y' which will be calculated from the 64 Fourier results by the LDA algorithm. In the more complex dataset explored below, 5 genotypes and 5 ages were sampled, leading to a multi-dimensional 'cloud' of data which can still be separated by a (more complex) set of linear equations.

Figure 3. We use the ERG to obtain accurate SSVEP measurements from both wild-type and PD Drosophila mutants at different contrasts and ages. In A-F we present exemplar ERG responses at 8Hz obtained from w^{-} and PINK1 PD mutants at 1 and 28 days of age, and at 64% and 99% contrast. SSVEP waveform peak amplitude increases with increasing contrast.

Figure 4: EOPD mutants show steeper response amplitudes at 1 day of age. A-E) Mean response amplitudes from all Drosophila genotypes (n=10 for each genotype). Drosophila exhibit visual tuning to temporal frequency and contrast, with peak sensitivity at 6-8Hz temporal frequency and 99% contrast. Further, the maps appear to show subtle differences outside of peak regions between 12-36Hz at 1-8% contrast. Profiles indicate that EOPD mutants have larger response amplitudes at 'peak sensitivity' regions. F) Boxplot of the 2f peak response at 99% contrast and 8Hz for each genotype.

Figure 5. High contrast (99%) and intermediate temporal frequency combinations (6-18Hz) conditions exhibit the strongest loading onto the first principal component. The entire dataset (N=250) is run through the PCA simultaneously to ensure that it is scaled by the same eigenvalue. Brighter colours represented a higher loading onto the first PC, whilst darker colours represent a lower loading.

Figure 6. One day old EOPD flies show increased SSVEP response amplitudes when compared to control flies (w^{-}). Mean PC Score (representing response

amplitude) as a function of age for five Drosophila genotypes (n=10 for each genotype/age group). Error bars show ±1SE.

Figure 7. All EOPD mutants show perturbations in response amplitudes after exposure to pulsating light, indicating a decrease in temporal contrast sensitivity (n=10 per genotype). A-E) Mean response amplitudes from all Drosophila genotypes after 7 days of visual stimulation (each genotype n=10, except DJ-1$\alpha^{\Delta 72}$ n=8). Same scale as Figure 3. F) Boxplot of the 2f peak response at 99% contrast and 8Hz.

Figure 8. Visual loss occurs in all PD mutants after 7 days of exposure to pulsating light. Mean PC Score of 5 Drosophila genotypes after 7 days exposure (each genotype n=10, except DJ-1$\alpha^{\Delta 72}$ n=8).

Figure 9. LDA can accurately discriminate between all 25 classes when they are included in the model. All classifications sit above 4% chance baseline, except for PINK1^{5} at 21 days of age.

Figure 10. Classification of young flies by genotypic class using data from temporal contrast response profiles. Mean classification accuracies for N-way LDA of 5 genotypes at 1 day of age (n=10 per genotype). The chance baseline is set at 20%, with mean classification accuracies between 45.5% and 78.8%.

Statistical Supplements

	w^-	DJ1-$\beta^{\Delta 93}$	DJ-1$\alpha^{\Delta 72}$	dLRRK^{ex1}
PINK1^5	p <. 001*	p = .724	p = .048*	p < .001*
w^-	-	p < .001*	p = .006*	p = .302
DJ1-$\beta^{\Delta 93}$	-	-	p = .892	p = .083
DJ-1$\alpha^{\Delta 72}$	-	-	-	p = .852

Table 1. Simple Effects Analysis: p-values at 1 day of age

	w^-	DJ1-$\beta^{\Delta 93}$	DJ-1$\alpha^{\Delta 72}$	dLRRK^{ex1}
PINK1^5	p = .208	p = .158	p = .185	p = .004*
w^-	-	p =.208	p = 1.000	p = 1.000
DJ1-$\beta^{\Delta 93}$	-	-	p = 1.000	p = .940
DJ-1$\alpha^{\Delta 72}$	-	-	-	p = .917

Table 2. Simple Effects Analysis: p-values at 7 days of age

	w^-	DJ1-$\beta^{\Delta 93}$	DJ-1$\alpha^{\Delta 72}$	dLRRK^{ex1}
PINK1^5	p = 1.000	p = .221	p = .042*	p = .019*
w^-	-	p = .064	p = .156	p =.080
DJ1-$\beta^{\Delta 93}$	-	-	p < . 001*	p < .001*
DJ-1$\alpha^{\Delta 72}$	-	-	-	p = 1.000

Table 3. Simple Effects Analysis: p-values at 14 days of age

	w^{-}	DJ1-$\beta^{\Delta 93}$	DJ-1$\alpha^{\Delta 72}$	dLRRK^{ex1}
PINK1^{5}	p = .897	p =.737	p = .440	p = .862
w^{-}	-	p = .052	p = .999	p =1.0
DJ1-$\beta^{\Delta 93}$	-	-	p = .006*	p = .042*
DJ-1$\alpha^{\Delta 72}$	-	-	-	p = 1.000

Table 4. Simple Effects Analysis: p-values at 21 days of age

	w^{-}	DJ1-$\beta^{\Delta 93}$	DJ-1$\alpha^{\Delta 72}$	dLRRK^{ex1}
PINK1^{5}	p = .515	p = 1.000	p = .010*	p = .275
w^{-}	-	p =.440	p = .753	p = 1.000
DJ1-$\beta^{\Delta 93}$	-	-	p = .007*	p =.222
DJ-1$\alpha^{\Delta 72}$	-	-	-	p = .937

Table 5. Simple Effects Analysis: p-values at 28 days of age

	7 days	14 days	21 days	28 days
1 day	p = .001*	p < .001*	p = .05*	p < .001*
7 days	-	p = .811	p = 1.000	p = 1.000
14 days	-	-	p = .372	p =.991
21 days	-	-	-	p = .951

Table 6. Simple Effects Analysis: p-values for w^{-} Drosophila

	7 days	14 days	21 days	28 days
1 day	p = 1.000	p = 1.000	p = 1.000	p = 1.000
7 days	-	p =.988	p = .938	p = .988
14 days	-	-	p = 1.000	p = 1.000
21 days	-	-	-	p = 1.000

Table 7. Simple Effects Analysis: p-values for DJ-1$\alpha^{\Delta 72}$ Drosophila

	7 days	14 days	21 days	28 days
1 day	p = .988	p = .005*	p = .691	p = .507
7 days	-	p < .001*	p = .178	p = .099
14 days	-	-	p = .427	p = .609
21 days	-	-	-	p = 1.000

Table 8. Simple Effects Analysis: p-values for DJ1-$\beta^{\Delta 93}$ Drosophila

	7 days	14 days	21 days	28 days
1 day	p = 1.000	p =1.000	p = .768	p = 1.000
7 days	-	p = 1.000	p = .698	p = 1.000
14 days	-	-	p = .923	p = 1.000
21 days	-	-	-	p = .634

Table 9. Simple Effects Analysis: p-values for PINK1^{5} Drosophila

	7 days	14 days	21 days	28 days
1 day	p = .998	p = .997	p = .852	p = .242
7 days	-	p = 1.000	p = .999	p = .733
14 days	-	-	p = .1.000	p = .806
21 days	-	-	-	p = .993

Table 10. Simple Effects Analysis: p-values for dLRRK^{ex1} Drosophila

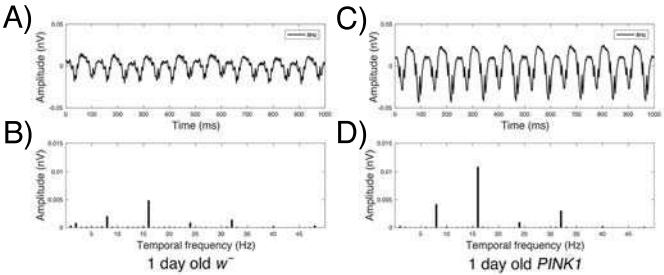
A)
C)
B)
D)
Amplitude (nV)
Time (ms)
Temporal frequency (Hz)
1 day old w⁻
1 day old PINK1

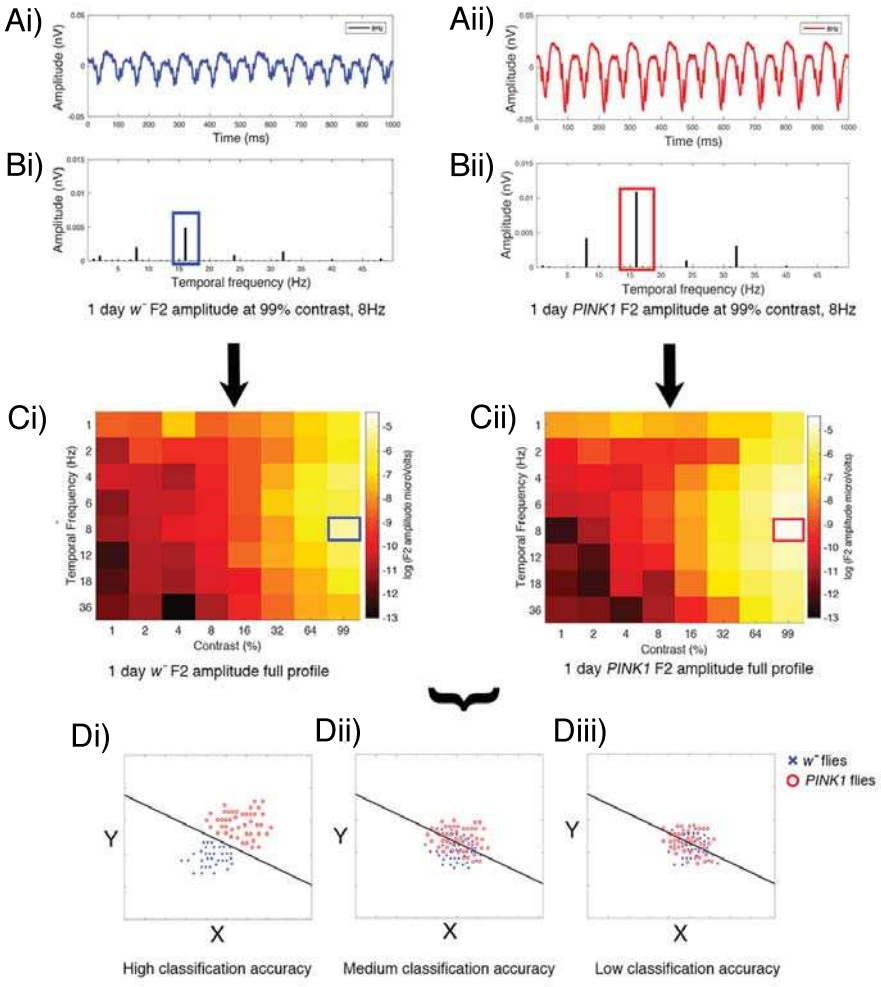
Ai)
Aii)
Amplitude (nV)
Time (ms)
Bi)
Bii)
Temporal frequency (Hz)
1 day w¯ F2 amplitude at 99% contrast, 8Hz
1 day PINK1 F2 amplitude at 99% contrast, 8Hz
Ci)
Cii)
Temporal Frequency (Hz)
Contrast (%)
log (F2 amplitude microVolts)
1 day w¯ F2 amplitude full profile
1 day PINK1 F2 amplitude full profile
Di)
Dii)
Diii)
w¯ flies
PINK1 flies
Y
X
High classification accuracy
Medium classification accuracy
Low classification accuracy

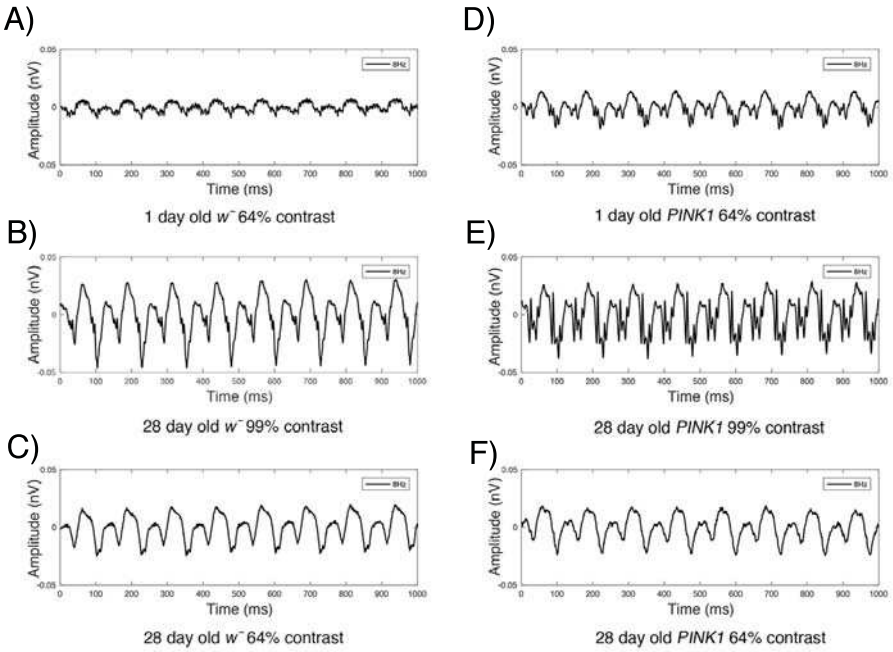
A)
Amplitude (nV)
Time (ms)
1 day old w¯ 64% contrast
B)
Amplitude (nV)
Time (ms)
28 day old w¯ 99% contrast
C)
Amplitude (nV)
Time (ms)
28 day old w¯ 64% contrast
D)
Amplitude (nV)
Time (ms)
1 day old PINK1 64% contrast
E)
Amplitude (nV)
Time (ms)
28 day old PINK1 99% contrast
F)
Amplitude (nV)
Time (ms)
28 day old PINK1 64% contrast

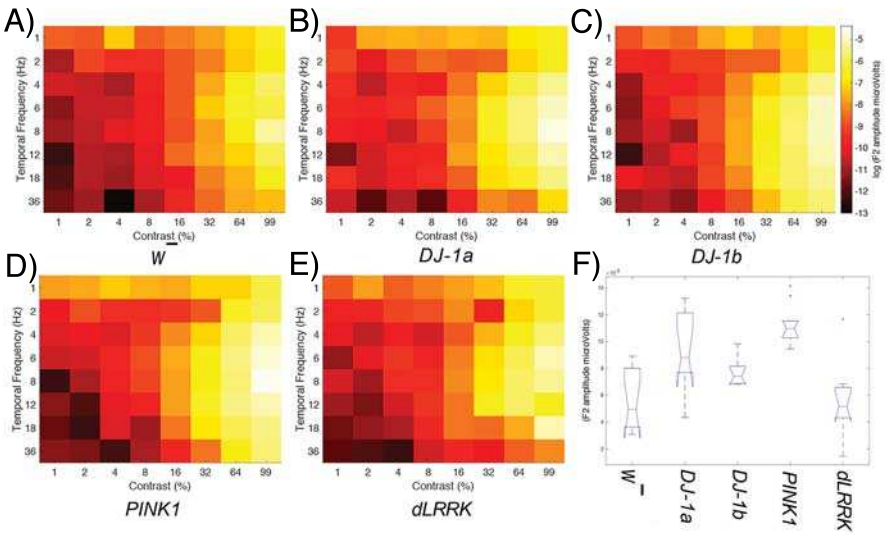
A)
B)
C)
D)
E)
F)
Temporal Frequency (Hz)
Contrast (%)
1 2 4 8 16 32 64 99
1 2 4 6 8 12 18 36
log (F2 amplitude microVolts)
-5 -6 -7 -8 -9 -10 -11 -12 -13
W1
DJ-1a
DJ-1b
PINK1
dLRRK
(F2 amplitude microVolts)
W1
DJ-1a
DJ-1b
PINK1
dLRRK

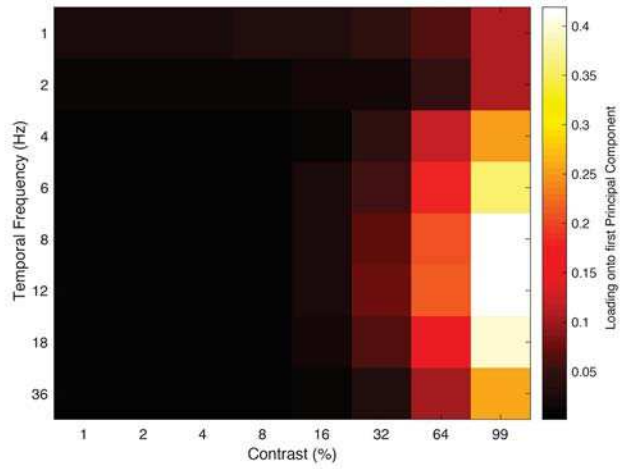
Temporal Frequency (Hz)
1
2
4
6
8
12
18
36
1
2
4
8
16
32
64
99
Contrast (%)
0.4
0.35
0.3
0.25
0.2
0.15
0.1
0.05
Loading onto first Principal Component

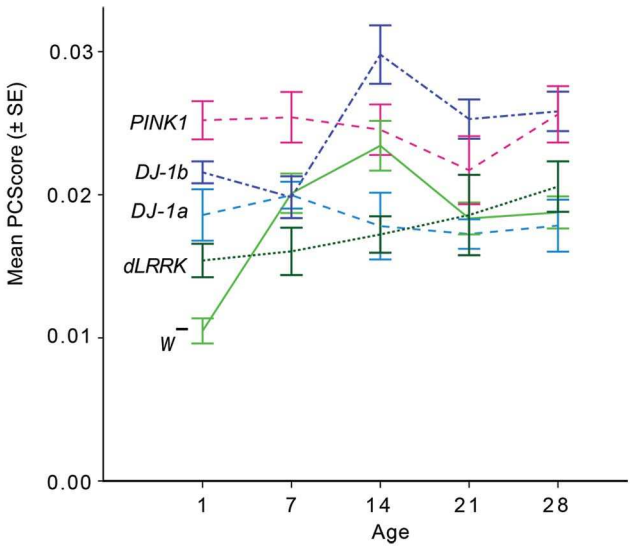
0.03
0.02
0.01
0.00
Mean PCScore (± SE)
PINK1
DJ-1b
DJ-1a
dLRRK
w⁻
1
7
14
21
28
Age

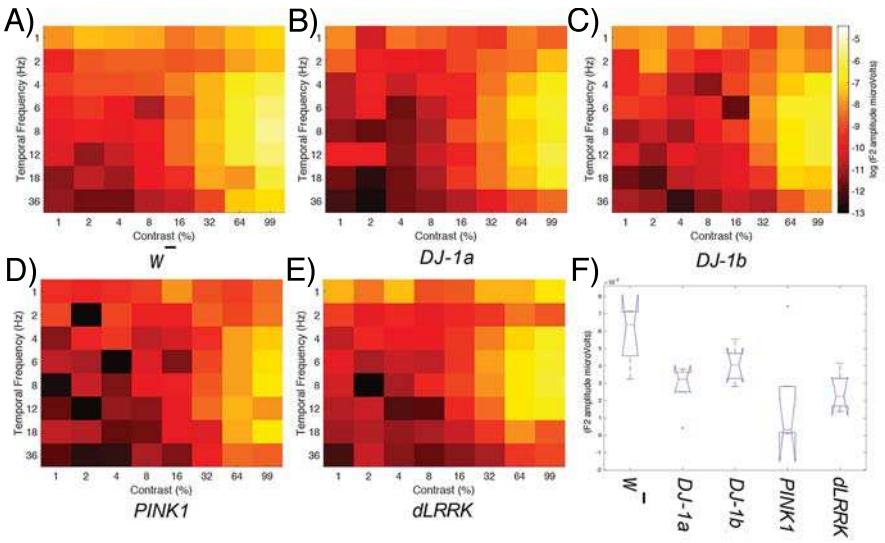
A)
B)
C)
D)
E)
F)
Temporal Frequency (Hz)
Contrast (%)
1 2 4 8 16 32 64 99
1 2 4 6 8 12 18 36
log of response amplitude
-5 -6 -7 -8 -9 -10 -11 -12 -13
w⁻
DJ-1a
DJ-1b
PINK1
dLRRK
(cPI2 amplitude microVolts)
w⁻
DJ-1a
DJ-1b
PINK1
dLRRK

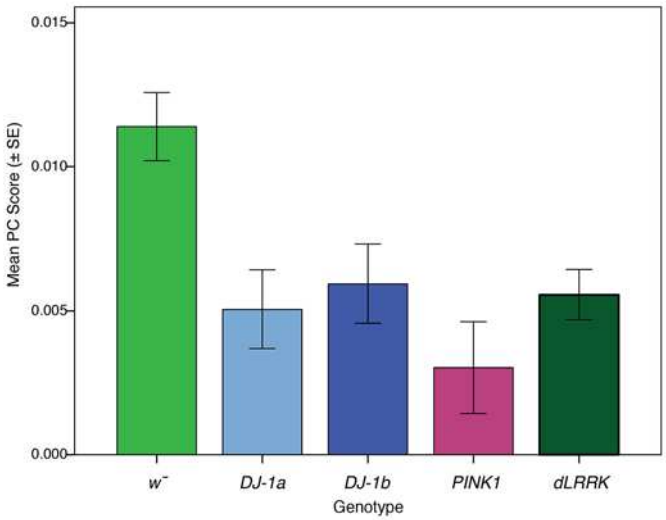
0.015
0.010
0.005
0.000
Mean PC Score (± SE)
w⁻
DJ-1a
DJ-1b
PINK1
dLRRK
Genotype

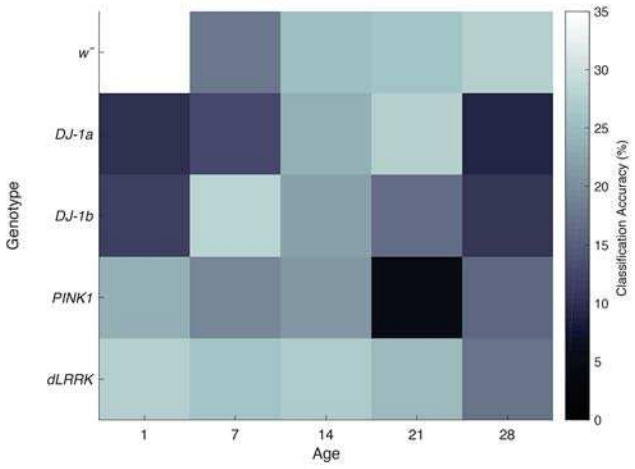
w^
DJ-1a
DJ-1b
PINK1
dLRRK
Genotype
1
7
14
21
28
Age
35
30
25
20
15
10
5
0
Classification Accuracy (%)

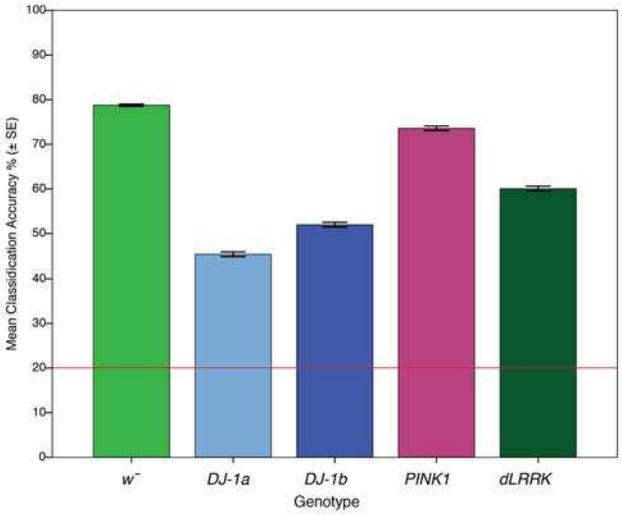
100
90
80
70
60
50
40
30
20
10
0
Mean Classidication Accuracy % (± SE)
w-
DJ-1a
DJ-1b
PINK1
dLRRK
Genotype